Dynamics and Control of the Tether Elevator/Crawler System

E. C. Lorenzini* and M. Cosmo†
Harvard-Smithsonian Center for Astrophysics, Cambridge, Massachusetts
and
S. Vetrella‡ and A. Moccia‡
Universita' di Napoli, Naples, Italy

This paper investigates the dynamics and acceleration levels of a new tethered system for micro- and variable-gravity applications. The system consists of two platforms tethered on opposite sides to the Space Station. A fourth platform, the elevator, is placed in between the Space Station and the upper platform. Variable-g levels on board the elevator are obtained by moving this facility along the upper tether, while microgravity experiments are carried out on board the Space Station. By controlling the length of the lower tether the position of the system center of mass can be maintained on board the Space Station despite variations of the system's distribution of mass. The paper illustrates the mathematical model, the environmental perturbations and the control techniques which have been adopted for the simulation and control of the system dynamics. Two sets of results from two different simulation runs are shown. The first set shows the system dynamics and the acceleration spectra on board the Space Station and the elevator during station-keeping. The second set of results demonstrates the capability of the elevator to attain a preselected g-level.

Introduction

CURRENT studies of microgravity experiments onboard the Space Station point out several requirements of such experiments that cannot be met by the microgravity laboratory presently designed for the Space Station. A variety of experiments, encompassing among others life sciences, material processes, and pharmaceutical research, have been proposed for the Space Station's microgravity laboratory. The threshold levels of acceleration noise for such experiments range from 10^{-2} to 10^{-8} g. A facility capable of exploring all or part of the range specified above would greatly enhance the capability of the Space Station in the area of microgravity. On the other hand such a system should not alter the acceleration level onboard the Space Station above the present requirement of 10^{-5} g (at all frequencies) in order to not interfere with the experiments to be carried out on the station.

The system that we propose consists of two end platforms (See Fig. 1), tethered to opposite sides of the Space Station. The upper and lower tethers have a diameter of 2 mm and a length of approximately 10 km. Since the upper and lower platforms are in a pollution-free environment (far from the station), they can be used for observation of the sky and the Earth respectively. The controlled gravity laboratory is located onboard a "space elevator" that can crawl along the upper tether between the Space Station and the upper platform. Microgravity experiments are carried out onboard a stationary laboratory (SML) that is attached to the transverse boom of the station. In order to minimize the gravity gradient acceleration onboard this laboratory, the center of mass (CM) of the system must be as close as possible to the stationary microgravity laboratory.[1] Consequently, the steady-state acceleration level onboard the elevator ranges from 1.5×10^{-5} to $4 \times 10^{-3} g$ as the elevator moves from the upper boom of the station to the tether tip, while the length of the lower tether is controlled in order to maintain the system CM at the SML.

This system has been called TECS, which stands for Tether Elevator/Crawler System.

The capability provided by the elevator will allow scientists to solve such major unresolved issues of microgravity science as experimental measurement of threshold values, the influence of g-jitters and hysteresis problems. Since TECS can maintain the system CM at the appropriate location by controlling the tether lengths, the elevator can maneuver along the tether without interfering with the microgravity experiments carried out on the station.

Description of the System

The system is formed by the Space Station with a mass of 306 metric tons and a frontal area of 2.7×10^3 m^2, by the elevator with a mass of 5 metric tons and a frontal area of 10 m^2, and by two end-platforms m_1 and m_4 with a mass of 10 metric tons and a frontal area of 10 m^2 each. The platforms are connected by 2-mm-diam Kevlar tethers with the thermal and mechanical characteristics listed in Table 1.

The distance between the SS and the upper platform is 10 km. The length of the lower tether is adjusted from 10 km to 15 km as a function of the position of EL along the upper tether in order to control the position of the system CM.

Several microgravity processes[1-3] require minimum acceleration levels ranging from 10^{-2} to 10^{-8} g at low frequencies. According to Refs. 1 and 2, the threshold levels of the acceleration for most of the proposed microgravity experiments exhibit a linear dependence upon the frequency for frequencies between 10^{-1} and 1 Hz; and a quadratic dependence above 1 Hz (see Fig. 2 derived from Ref. 1). As shown in Fig. 2, microgravity processes are mostly sensitive to disturbances with frequency smaller than 10^{-3} Hz. Consequently, external perturbations with a frequency content comparable to the orbital frequency, such as acceleration terms generated by aerodynamic forces and J_2 gravity components, strongly affect the microgravity experiments.

On the other hand, the noise arising from among others, structural vibrations, crew motion, vernier thrusters for atti-

Paper presented at the PSN/NASA/ESA/AIDAA/AIAA/AAS Second International Conference on Tethers in Space, Venice, Italy, Oct. 4–8, 1987. Received Nov. 10, 1987, revision received March 14, 1988.

*Staff Scientist, Radio and Geoastronomy Division.
†Visiting Scientist, Radio and Geoastronomy Division.
‡Chair of Aerospace Systems Engineering.

tude control and spacecraft dockings, usually called g-jitters, have frequencies greater than 10^{-3} Hz, and are less of a problem according to Fig. 2.

In addition, longitudinal vibrations of the tethers are excited by thermal shocks, which take place at the crossing of the terminator. Given the actual mechanical characteristics and lengths of the tethers of our system, these oscillations, also called thermal g-jitters, have a frequency range from 10^{-3} to 10^{-2} Hz. According to Fig. 2, those are of intermediate importance to the microgravity experiments.

In the next sections we will address the impact of TECS on the acceleration level onboard the Space Station. We will also evaluate the acceleration fluctuations, onboard the elevator, caused by environmental perturbations with respect to scientific requirements.

Table 1 Characteristics of Kevlar tether

Young's modulus	1.96×10^{10} N/m^2
Absorptivity, α	0.75
Emissivity, ε	0.5
Specific heat	2500 J/Kg-K
Linear density	4.85×10^{-3} Kg/m
Coefficient of thermal expansion	-2×10^{-6} K^{-1}

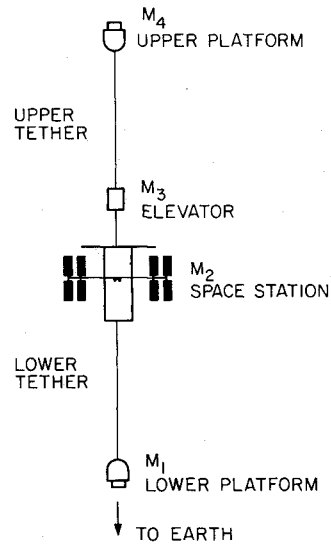

Fig. 1 Schematic of tether elevator/crawler system.

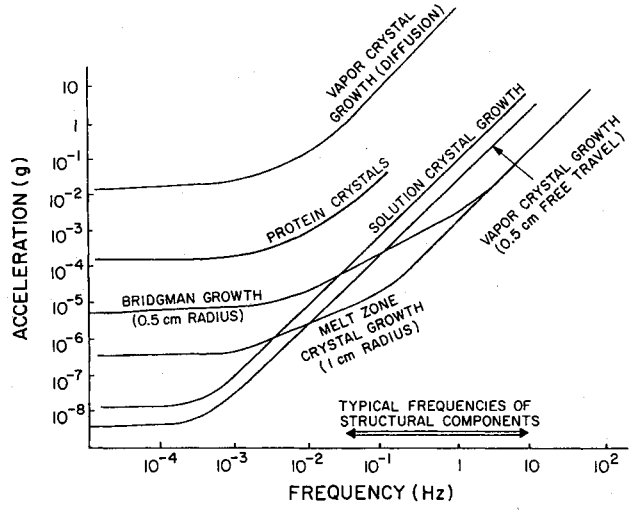

Fig. 2 Acceleration sensitivity of material processes.[1]

Mathematical Model

Equations of Motion

The motion of this tethered system is described with respect to an orbiting reference frame (ORF) that rotates at constant orbital rate Ω and radius R_0. The origin of this frame coincides with the initial position of the system CM (see Fig. 3). The x axis is along the ORF velocity vector, the z axis is along the local vertical toward the Earth, and the y axis completes the right-handed reference frame.

An Earth-centered inertial reference frame (IRF) is also erected. The X axis points toward the vernal equinox, the Z axis points toward the North Pole and the Y axis completes the right-handed reference frame.

The three-dimensional mathematical model, adopted for our analysis, has been developed according to the following assumptions: lumped masses, elastic tethers and generic orbit of the system.[4,5]

If we denote $\boldsymbol{r}_i$ as the position vector of the ith mass m_i with respect to ORF, $\boldsymbol{F}_{g,i}$, $\boldsymbol{F}_{d,i}$ and $\boldsymbol{F}_{T,i}$ as the gravity, drag, and tensional forces acting respectively upon the ith mass, the equations of motion of the N masses of the system in vectorial form are

$$\ddot{\boldsymbol{r}}_i = -\ddot{\boldsymbol{R}}_0 - 2\boldsymbol{\Omega} \times \dot{\boldsymbol{r}}_i - \boldsymbol{\Omega} \times (\boldsymbol{\Omega} \times \boldsymbol{r}_i)$$

$$+(1/m_i)(\boldsymbol{F}_{g,i} + \boldsymbol{F}_{d,i} + \boldsymbol{F}_{T,i}), \qquad i = 1,...,N \tag{1}$$

where the prime denotes derivation with respect to time. Equations (1) are a set of N vectorial equations or correspondingly a set of $3 \times N$ scalar equations that have to be integrated numerically in order to obtain the motion of the system.

Environmental Models

Because of the very low acceleration levels in which we are interested, an accurate model of external forces is necessary in order to simulate with high enough fidelity the effects of the environment on the system dynamics. The external perturbations considered in the present analysis are the gravitational forces $\boldsymbol{F}_g$, the aerodynamic forces $\boldsymbol{F}_d$, and the thermal effects on the tensional forces $\boldsymbol{F}_T$.

Unlike other tether simulation models,[6,7] our gravity model is not linearized and takes into account the second zonal harmonic of the gravity field (J_2 term). The J_2 term has a secular effect on such orbital parameters of the system as mean anomaly, argument of perigee, and right ascension of the ascending node. The J_2 term also affects the librations and lateral oscillations (see next section) of a long multimass tethered system such as the one under analysis.

The drag model is an analytical fit of Jacchia's 1977 density model.[8,9] The atmospheric density varies as a function of the altitude (the Earth's oblateness is also considered) and the local exospheric temperature. The latter takes into account the diurnal variation, which is a function of local solar time, latitude, and solar activity.

The thermal inputs on the tether segments are the solar illumination, the Earth's albedo, and the infrared Earth radiation. The only cooling process is the emitted radiation. The position of the terminator is computed as a function of the Sun's position along the ecliptic. As the system crosses the terminator, the tether temperature varies abruptly; consequently, the tether segments expand or contract and the tethers' tensions exhibit steep variations. The $N-1$ equations of the thermal balance of the tether segments are added to

Eqs. (1). The thermal equation of the jth tether segment is given by

$$\dot{T}_j = \frac{2r_j\alpha_j I^{\text{sun,inc}} + aI^{\text{sun}}\alpha_j r_j f_j \cos\gamma_j + 2\pi r_j \sigma\bar{\alpha}_j f_j T_\oplus^4 - 2\pi r_j \sigma\varepsilon_j T_j^4}{\rho_j c_j \pi r_j^2}$$

$$j = 1,\ldots,N-1 \qquad (2)$$

where

a = Earth albedo (annual average)
c_j = specific heat of jth tether
f_j = view factor of jth tether
I^{sun} = solar flux
$I^{\text{sun,inc}}$ = solar flux incident on tether
I^{sun} and $I^{\text{sun,inc}}$ are equal to zero during the eclipses
r_j = radius of jth tether
T_j = temperature of jth tether
$T_\oplus$ = Earth temperature
α_j = absorbitivity of jth tether
$\bar{\alpha}_j$ = infrared absorbitivity of jth tether
ε_j = emissivity of jth tether
γ_j = sun zenith angle of jth tether
σ = Stefan-Boltzmann constant
ρ_j = volume density of jth tether

System Dynamics

Degrees of Freedom

The coordinates x_i, y_i, z_i of the point masses with respect to the ORF are numerically integrated by the computer code with a fourth-order Runge-Kutta or a predictor-corrector integration routine.

A second set of coordinates has also been selected in order to provide a more direct description of the system dynamics. This set of coordinates is formed by (see Fig. 3): the in-plane (in the orbital plane) θ and out-of-plane (orthogonal to the orbital plane) φ angles of libration between the line connecting the end-masses and the local vertical through the system CM; the $N-1$ lengths of tether segments ℓ_i, where N is the number of the lumped masses and the $N-2$ lateral deflections ε_i of the inner masses with respect to the line through the end-masses. The coordinates ε_i are further projected onto the in-plane ε_{Ii} and out-of-plane components ε_{Oi}.

This set of parameters identifies such characteristic oscillations of the system as the low frequency f librations ($f \simeq 10^{-4}$ Hz), the medium frequency lateral oscillations ($f \simeq 10^{-3}$ Hz), and the higher frequency longitudinal oscillations ($10^{-3}\ Hz < f < 10^{-2}$ Hz).

Accelerations

The acceleration measured by an accelerometer package onboard any platform of the system is the sum of the external, excluding the gravitational, and internal forces (e.g., tensions) acting upon a platform divided by the mass of that platform. Since the platforms librate approximately like the overall tethered system, an accelerometer package onboard a platform (e.g., the elevator) does not measure the orthogonal components of the acceleration caused by the librations (as an accelerometer package on a pendulum measures zero along the axes orthogonal to the pendulum).

First we erect the orbiting reference frame $x_{CM}y_{CM}z_{CM}$ (CMRF) that is like the previously defined ORF except for the origin of CMRF which coincides with the instantaneous CM of the system. Since the attitude dynamics of the individual platforms are not modeled in the present code, the best approximation to a body reference frame is the system-body reference frame (SBRF). This frame of coordinates is rotated by the two angles θ and φ with respect to the CMRF (see Fig. 3). The accelerations measured onboard the Space Station and the space elevator are projected onto the SBRF whose components are the most meaningful for the experimenter. The acceleration components of the SBRF are as follows: the front component along the x_{SB} axis, the side component along the y_{SB} axis, and the longitudinal component along the z_{SB} axis.

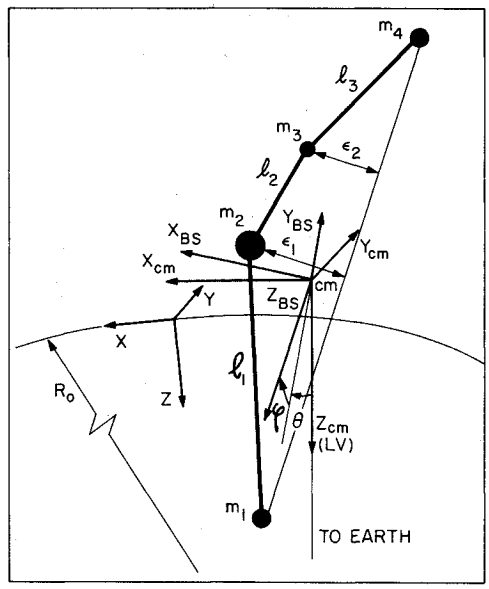

Fig. 3 Reference frames.

Damping of Oscillations

The system has several oscillations, associated with some of its degrees of freedom, that can affect the "quality" of the accelerations measured on board the Space Station and the space elevator.

As pointed out in previous papers,[10,11] the tethers introduce a "noise" at the longitudinal vibration frequencies that may impair the performance of the system. Lateral deflections and longitudinal oscillations also have a nonnegligible effect on the accelerations on board the elevator.

At the orbital inclination of 28.5 deg the in-plane perturbations are much stronger than the out-of-plane perturbations. In-plane oscillations, furthermore, are excited by Coriolis forces during transient maneuvers of the system (e.g., deployment and crawling maneuvers), while out-of-plane oscillations are not. Luckily the in-plane oscillations are much easier to damp out by means of tether control than the out-of-plane oscillations.

This section explains briefly the strategy that we adopt for damping the in-plane oscillations by controlling the lengths of the tethers. A more thorough treatment of this rather complex topic, which is beyond the scope of this paper, will be presented in a future paper.

Damping of longitudinal tether vibrations is provided by passive (spring-dashpot systems in series with each tether segment) or active (reel control) dampers. The latter is the most likely mechanization of the longitudinal dampers because a passive damper would be required to stretch tenths of meters. In the active case, the ith reel controls the tension of the associated tether segment with a proportional-derivative control law. The ith control law is tuned to the frequency of the longitudinal oscillations of the ith tether segment. The derivative term is such as to provide a damping ratio of 90% of the critical value which provides an effective damping of the longitudinal (spring-mass mode) oscillations.

The in-plane libration and the in-plane lateral oscillations are damped out by exploiting the Coriolis forces. The reels control the tether lengths with terms proportional to the libration angle θ and the in-plane components of the lateral deflections ε_{Ii} in such a way as to extract energy from the above mentioned oscillations. In-plane Coriolis forces have a

strong coupling with the displacements of the platforms in the orbital plane. An effective damping of the libration and of the lateral oscillations can be obtained by controlling the tether lengths in opposition to the oscillations to be damped out.

As a conclusion to this section we wish to point out that the longitudinal dampers must be activated throughout the mission in order to damp out the oscillations arising from the thermal shocks. The in-plane dampers, on the contrary, are only necessary during transient phases (e.g., deployment and crawling maneuvers). The in-plane dampers, however, can be conservatively activated during steady-state phases (e.g., station-keeping) in order to improve (slightly) the performance during such phases. Out-of-plane dampers are not necessary under normal conditions. Active thrusters could be used sporadically under emergency conditions.

Elevator's Control

The most peculiar feature of TECS is the capability of the elevator to crawl along the upper tether in order to produce an assigned g profile vs time onboard the elevator. One of these maneuvers consists of moving the elevator from its initial location, and consequently initial g level, to a final position with a different g level. This maneuver is usually called g tuning and it is designed for exploring acceleration thresholds of microgravity experiments.

A control law, suitable for this maneuver, must meet the following requirements: 1) acceleration and deceleration phases as smooth as possible, 2) small perturbations of the system dynamics, and 3) capability of maintaining the acceleration level onboard the Space Station below 10^{-5} g.

Toward this end we derived a modified hyperbolic tangent control law[11] (MHT) with the addition of a constant velocity phase.[12] The constant velocity phase starts at the end of the acceleration phase when the maximum velocity is reached, and the acceleration is equal to zero. The hyperbolic tangent is resumed at the end of the constant velocity phase to decelerate the elevator. Since the hyperbolic tangent is asymptotic, a cut-off distance σ from the target point on the tether has been adopted in order to limit the total travel time. In terms of the variation of the traveled tether length $\Delta\ell_c$ vs time, the control law for the elevator's motion can be expressed as follows:

Acceleration

$$t < t_A$$

$$\Delta\ell_c = \Delta\ell'_c[\tanh(\alpha t)]^\gamma \tag{3a}$$

Constant Velocity

$$t_A \le t < t_B$$

$$\Delta\ell_c = \Delta\ell'_c[\tanh(\alpha t_A)]^\gamma + \Delta\ell''_c \frac{t - t_A}{t_B - t_A} \tag{3b}$$

Deceleration

$$t_B \le t \le t_\sigma$$

$$\Delta\ell_c = \Delta\ell'_c\{\tanh\alpha[t - (t_B - t_A)]\}^\gamma + \Delta\ell''_c \tag{3c}$$

where

$\Delta\ell'_c$ = tether length traveled during acceleration plus tether length traveled during deceleration
$\Delta\ell''_c$ = tether length traveled during the constant-velocity phase
t_A = time at which the maximum velocity is reached
t_B = time at the end of the constant-velocity phase
t_σ = time at the cut-off distance σ from the target point
α = rate parameter
γ = shape parameter

The ratio of the tether length traveled during acceleration plus deceleration to the total length traveled is the dimensionless parameter χ. Calling the total length traveled $\Delta\ell_{cT}$, we have

$$\Delta\ell_{cT} = \Delta\ell'_c + \Delta\ell''_c \tag{4a}$$

$$\Delta\ell'_c = \chi\Delta\ell_{cT} \tag{4b}$$

$$\Delta\ell''_c (1 - \chi)\Delta\ell_{cT} \tag{4c}$$

By using the three control parameters α, γ, and χ, the total travel time, the maximum crawling velocity, and the acceleration profile vs time can be conveniently adjusted to meet the first two requirements. The transition between two sequential segments of the control law is smooth since the acceleration has no discontinuity (specifically the acceleration is equal to zero at transition). Consequently, the elevator crawls along the tether according to three sequential and smoothly continuous phases.

In order to meet the third requirement, the lower reel controls the lower tether according to Eq. (3), where the length variations $\Delta\ell'_c$ and $\Delta\ell''_c$ have been scaled down by the factor m_3/m_1. Because of this compensatory control, the system CM is maintained very close to its initial position during the elevator's maneuver.

Since a long Kevlar tether is highly deformable, the total traveled length $\Delta\ell_{cT}$ must be corrected for the elastic deformation of the tether if the desired final distance between the Space Station and the elevator is to be attained with good accuracy. This corrective term is easily computed before starting the maneuver.

As a result of a parametric analysis of the MHT control law, we found that for a typical long-distance-maneuver (e.g., $\Delta\ell_{cT} = 4$ km) an appropriate choice of the control parameter is $\alpha = 10^{-3}$ s^{-1}, $\gamma = 4$, and $\chi = 0.2$. The cut-off distance σ was assumed equal to 1 m. The results of a simulation run, in which the elevator maneuvers according to Eqs. (3) and the previously selected control parameters, is shown later on in this paper.

Numerical Results

Station-Keeping

The first set of numerical results are relevant to a station-keeping simulation run. The system is initially at rest and aligned with LV. The elevator is at 1 km from the Space Station and the lower tether is 10.5 km long. The sun is at the summer solstice and the initial tether temperature is 290 K for all tether segments. All the environmental perturbations modeled in our code are acting upon the system. The longitudinal and in-plane lateral/librational dampers are activated during the entire simulation run. The duration of the simulation run is 20 orbits in order to show the very long frequency beating phenomena. The Space Shuttle orbits at an initial altitude of 450 km and an inclination of 28.5 deg. The orbital period is equal to 5615 s.

The acceleration components measured onboard the Space Station and the relative spectra are depicted in the following figures: the front component and its spectrum in Figs. 4a and 4d; the side component and its spectrum in Figs. 4b and 4e; the longitudinal component and its spectrum in Figs. 4c and 4f. None of the spectra of this section show the dc components that have been removed from the acceleration components before computing the fast Fourier transforms.

The amplitudes of the front and side accelerations are of the order of 10^{-8} g. The amplitudes are influenced by the librations and their coupling with the lateral oscillations. In particular, the side component shows a beating phenomenon between the out-of-plane libration and the out-of-plane lateral oscillations. The spectrum of the front acceleration component (Fig. 4d) shows a main harmonic at the orbital frequency

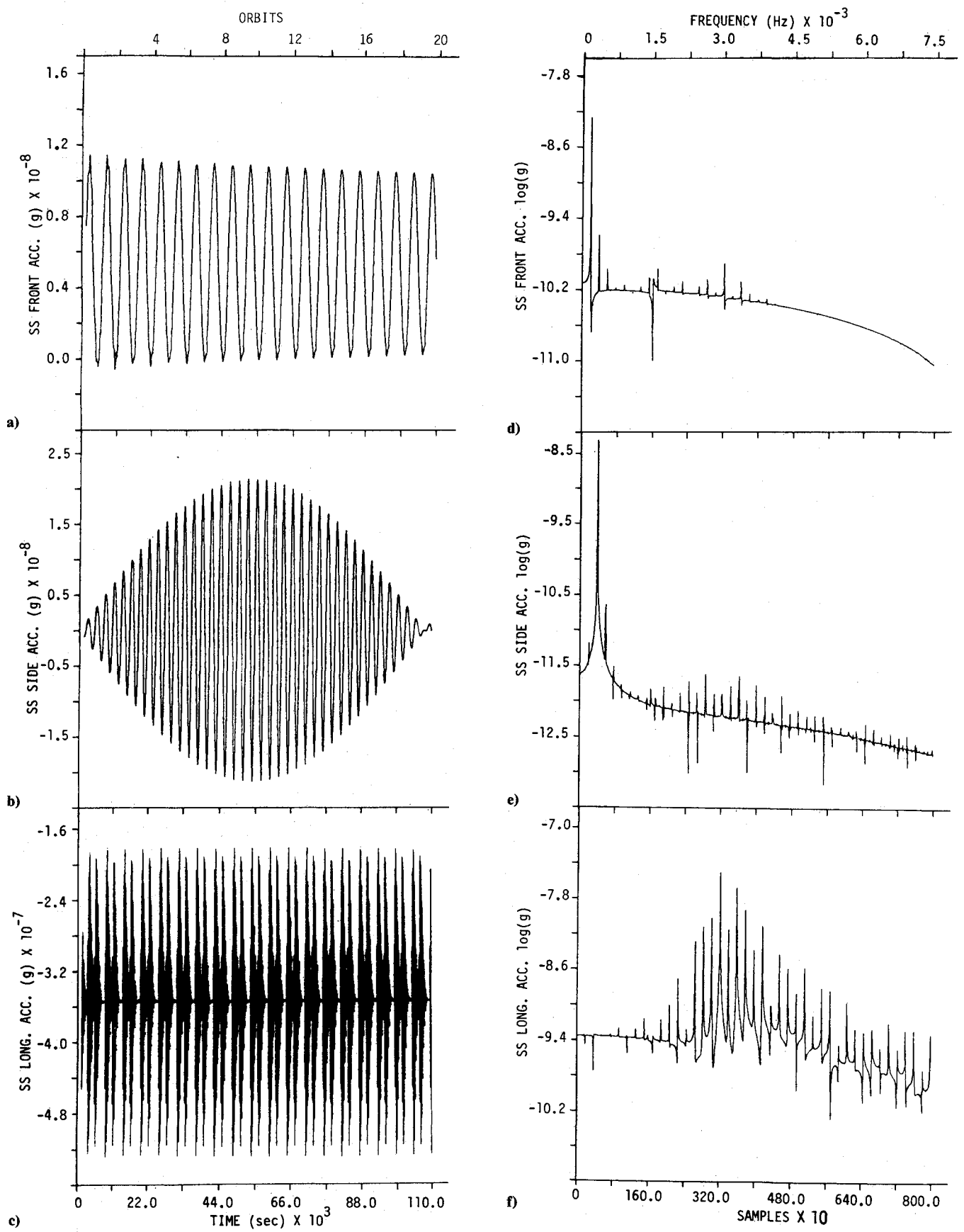

Fig. 4 Space Station acceleration components: a) front, b) side, and c) longitudinal. Space Station acceleration spectra: d) front, e) side, and f) longitudinal.

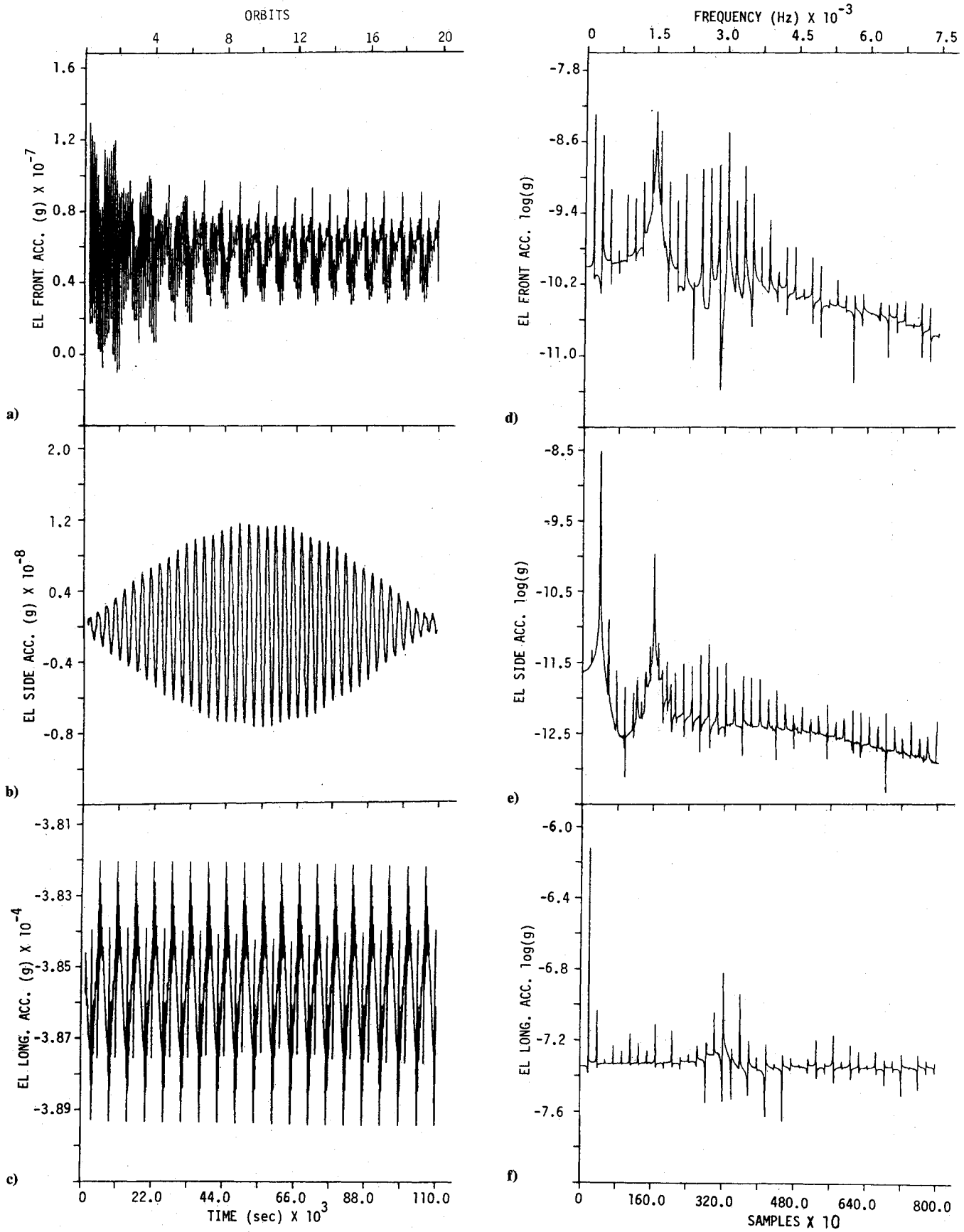

Fig. 5 Elevator acceleration components: a) front, b) side, and c) longitudinal. Elevator acceleration spectra: d) front, e) side, and f) longitudinal.

($f = 1.8 \times 10^{-4}$ Hz) and a smaller harmonic at twice the orbital frequency, both caused by the J_2 gravity term and the drag. In particular the Space Station accounts for the major contribution to the drag. The spectrum of the lateral acceleration component (Fig. 4e) shows two harmonics at the same frequencies as the previous case but with inverted amplitudes.

The longitudinal acceleration exhibits a dc component of $3.6 \times 10^{-7}\,g$ arising from the offset between the system CM and the orbital center (the zero acceleration point of the system). This dc component can be eliminated by adjusting the length of the lower tether in order to place the orbital center at the SML onboard the Space Station where the acceleration is measured. In this simulation run, however, we have decided to show the effect of the above-mentioned offset upon the acceleration level onboard the SML. The longitudinal acceleration component exhibits relatively strong thermal jitters, which are caused by the crossing of the terminator and are subsequently abated by the in-line dampers (Fig. 4c). The spectrum of the longitudinal acceleration component in Fig. 4f shows frequencies, higher than the orbital frequency, of approximately 3×10^{-3} Hz, which are typical of longitudinal oscillations (excited by thermal shocks).

This analysis demonstrates, within the assumptions of our model, that TECS provides a negligible contribution to the acceleration noise onboard the Space Station.

The acceleration components measured onboard the elevator and the relative spectra are depicted in the following set of figures: the front component and its spectrum in Figs. 5a and 5d; the side component and its spectrum in Figs. 5b and 5e; and the longitudinal component and its spectrum in Figs. 5c and 5f. The front and side components show harmonics at the orbital frequency and at twice the orbital frequency that are caused by the J_2 term and by the drag. The drag also accounts for the dc component of the front acceleration. The higher frequency harmonics in the spectra are generated by thermal shocks. The orders of magnitude of the fluctuations of the front and side components are 10^{-7} and $10^{-8}\,g$, respectively.

The longitudinal acceleration component is shown in Fig. 5c. The longitudinal acceleration has a dc component of $-3.86 \times 10^{-4}\,g$, which is provided by the gravity gradient caused by the offset between the EL and the orbital center. The harmonic at the orbital frequency (see Fig. 5f), with an amplitude of the order of $10^{-6}\,g$, is caused by the J_2 gravity term. The J_2 component forces the system to librate, hence

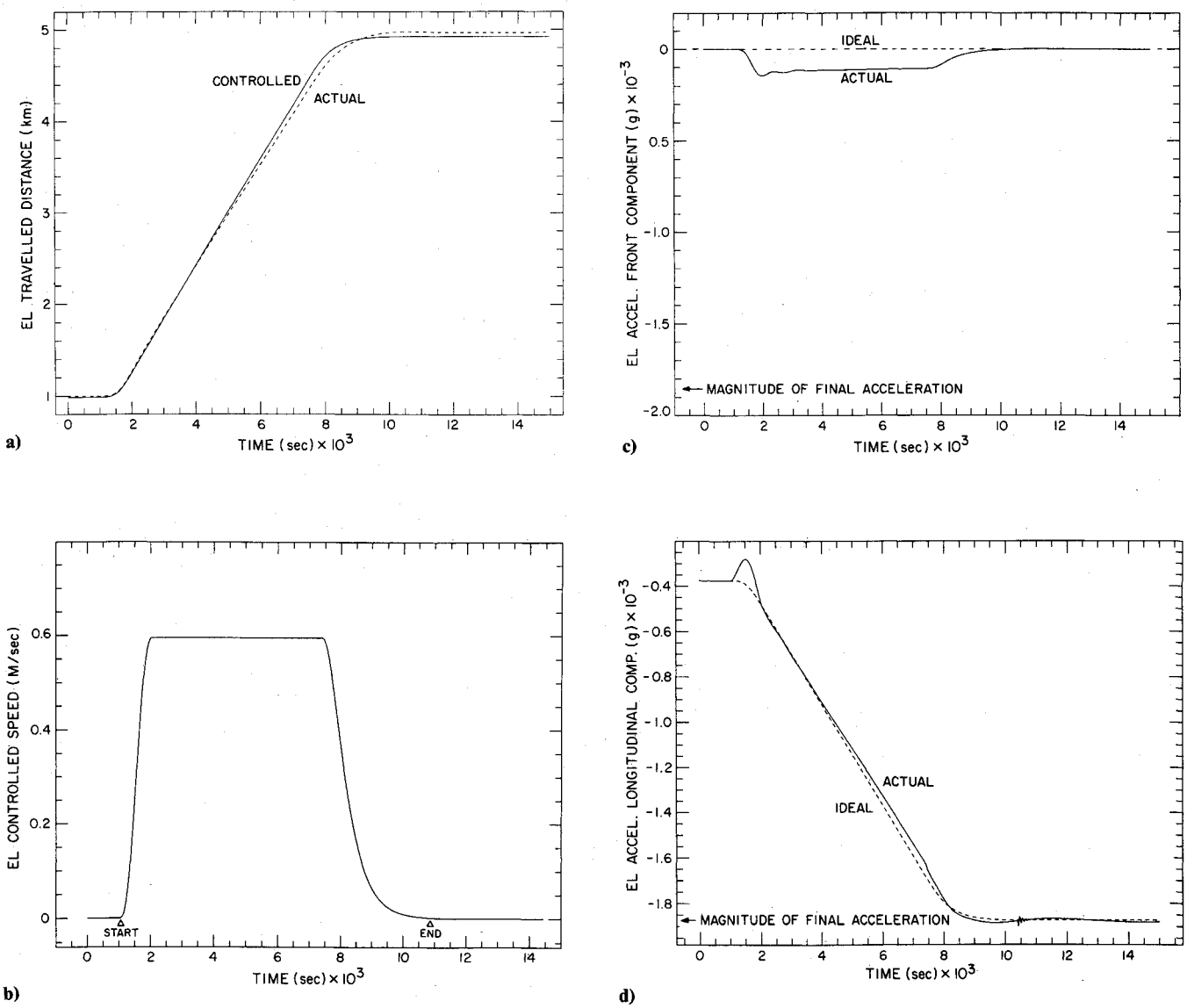

Fig. 6 Dynamics properties of elevator during a crawling maneuver: a) distance, b) speed, c) front acceleration, and d) longitudinal acceleration.

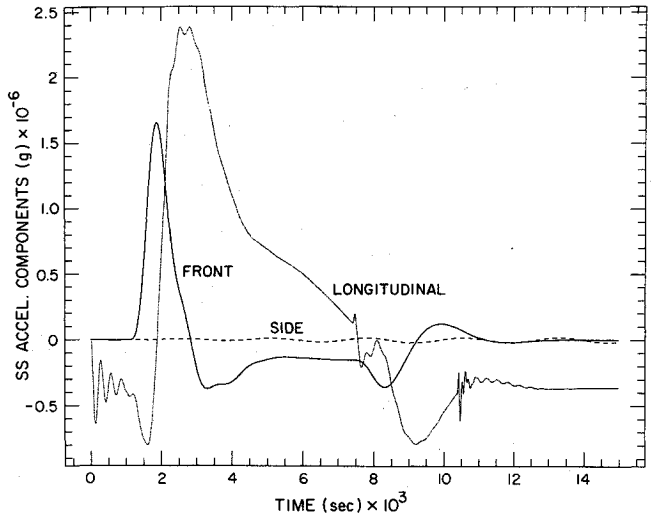

Fig. 7 Acceleration components onboard the Space Station.

stretching the tethers with the libration frequency. The tether tensions produced by this mechanism balance out at the system CM. Since the elevator is offset from the CM, the J_2-induced tether tensions apply a differential force to the elevator, which accounts for the spectral line at the orbital frequency. The higher-frequency harmonics of the longitudinal acceleration component are centered around the longitudinal natural frequency of the upper tether system. These higher-frequency components are generated by thermal shocks.

Crawling Maneuvers

We show in this section the results of a typical crawling maneuver. The system is initially at rest and aligned with LV. At time $t = 1000$ s the elevator starts moving, according to Eqs. (3), from the initial distance of 1 km from the Space Station to the final distance of 5 km from the Space Station. The control parameters are those selected in the previous section. At the same time, the length of the lower tether is controlled in order to compensate for the elevator's displacement. In this case the thermal perturbations are negligible with respect to the variations of the acceleration level and therefore have been neglected.

The actual distance from the Space Station and the controlled distance traveled by the elevator are depicted in Fig. 6a. The elevator-controlled velocity is shown in Fig. 6b. The front and longitudinal acceleration components onboard the elevator are shown in Figs. 6c and 6d. Both the acceleration components onboard the elevator are compared to the respective unperturbed components (ideal case of an elevator that moves without perturbing the system). The front component during the maneuver is affected by the Coriolis force, while the longitudinal component is mostly affected by the elasticity of the system. The side acceleration component is not shown, because it is negligible with respect to the other components.

The acceleration components onboard the elevator, of which the longitudinal component is the greatest, have a behavior close to the ideal and achieve smoothly the steady-state values at the end of the crawling, as required by a g-tuning type of maneuver.

The acceleration components onboard the Space Station, along the SBRF, are depicted in Fig. 7. Since the lower platform is controlled in such a way as to balance the elevator's motion, the acceleration level onboard the Space Station are well within the requirement for microgravity experiments.

Conclusions

The proposed tethered system supplements the Space Station with a facility for carrying out experiments in a controlled gravity environment. The acceleration level onboard the elevator can be tuned between 1.5×10^{-5} and $4 \times 10^{-3}\,g$, making possible the exploration of threshold acceleration levels for several experiments proposed by the microgravity scientific community.

The "quality" of the acceleration onboard the elevator is as follows: the longitudinal component is the most critical, with harmonic components of $10^{-6}\,g$ at frequencies lower than 10^{-3} Hz and of $10^{-7}\,g$ for frequencies between 10^{-3} and 10^{-2} Hz. The front component of the acceleration depends primarily on the drag of the Space Station and ultimately on its configuration. The side component of the acceleration is negligible. The quality of the acceleration onboard the elevator is therefore better than onboard the stationary microgravity laboratory of the Space Station.

This tethered system moreover, can control the vertical position of the system center of mass despite a modification of the system's configuration. In particular, we have demonstrated the system's capability of maintaining the acceleration level on the station within the microgravity requirements, notwithstanding the elevator's maneuvers along the upper tether in performing g-tuning experiments.

The proposed system does not have an appreciable impact on the acceleration level onboard the Space Station. The tethered-system-related noise is a few orders of magnitude less than the $10^{-5}\,g$ acceleration level specified for the station.

Acknowledgments

This paper has been supported in the United States by NASA/MSFC Contract NAS8-36606, with James Harrison and Chris Rupp as Program Directors, and in Italy by PSN/CNR Contract. The authors would also like to thank Ms. Catherine Mannick for the help provided in editing the paper.

References

[1]Sharpe, A. (ed), "Low Acceleration Characterization of Space Station Environment," Teledyne Brown Engineering, Final Rept. for NASA/MSFC Contract NAS8-36122, Mod. 6,Oct. 1985.

[2]Baugher, C. R. (ed), "Micro-g Requirements Analysis, Space Station RUR-2," EMS Product, Rept. for NASA/MSFC, WPO1, EMS R5.1.4, Aug. 1985.

[3]Carruthers, J. R., "Acceleration Level Requirements for Microgravity Science on the Space Station," INTEL, Rept. for NASA/MSFC, May 1985.

[4]Kalaghan, P. M., Arnold, D. A., Colombo, G., Grossi, M. D., Kirshner, L. R., and Orringer, O., "Study of the Dynamics of a Tethered Satellite System (SKYHOOK)," Smithsonian Astrophysical Observatory Final Rept. for NASA/MSFC, Contract NAS8-32199, March 1978.

[5]Lang, D. D., "TOSS Reference Manual," NASA NAG9-16715, Vol. 1, May 1985.

[6]Baker, P. W., Dunkin, J. A., Galabott, Z. J., Johnston, K. D., Kissel, R. R., Rheinfurt, M. H., and Siebel, M. P. L., "Tethered Subsatellite Study," NASA TMX-73314, March 1976.

[7]Spencer, T. M., "Atmospheric Perturbation and Control of a Shuttle/Tethered Satellite," *Proceedings of the Eighth IFAC Symposium,* edited by C. W. Munslay, Pergamon, New York, 1980.

[8]Roberts, C. E., "An Analytical Model for Upper Atmosphere Densities Based Upon Jacchia's 1970 Models," *Celestial Mechanics,* Vol. 4, 1971, pp. 368–377.

[9]Jacchia, L. G., "Thermospheric Temperature, Density and Composition: New Models," Smithsonian Astrophysical Observatory, Cambridge, MA, Rept. SR375, March 1975.

[10]Lorenzini, E. C., "A Three-Mass Tethered System for Micro-g/Variable-g Applications," *Journal of Guidance, Control, and Dynamics,* Vol. 10, May–June 1987, pp. 242–249.

[11]Lorenzini, E. C., "Artificial Gravity Laboratory," *Tether Dynamics Simulation,* NASA CP 2458, pp. 141–160, 1987.

[12]Swenson, F. R., "Tether Crawler System," Tri-State Univ., Angola, IN, Rept. for NASA-MSFC, Contract NGT 01-002-099, Aug. 1986.